Are petrous bones just a repository of ancient biomolecules? Investigating biosystematic signals in sheep petrous bones using 3D geometric morphometrics

Camille Bader, Christophe Mallet, Jwana Chahoud, Agraw Amane, Bea de Cupere, Remi Berthon, Franck Lavenne, Azadeh Mohaseb, Hossein Davoudi, Moussab Albesso, et al.

Journal of Archaeological Science: Reports 43 (2022) 103447

Contents lists available at ScienceDirect

Journal of Archaeological Science: Reports

journal homepage: www.elsevier.com/locate/jasrep

Are petrous bones just a repository of ancient biomolecules? Investigating biosystematic signals in sheep petrous bones using 3D geometric morphometrics

Camille Bader [a,b], Christophe Mallet [b], Jwana Chahoud [c,d], Agraw Amane [e,j,k], Bea De Cupere [f], Remi Berthon [a], Franck Lavenne [g], Azadeh Mohaseb [a,h], Hossein Davoudi [h], Moussab Albesso [c], Homa Fathi [h], Manon Vuillien [a], Joséphine Lesur [a], Daniel Helmer [c], Lionel Gourichon [i], Olivier Hanotte [j,l], Marjan Mashkour [a,h], Emmanuelle Vila [c], Thomas Cucchi [a,*]

[a] Archéozoologie, Archéobotanique: Sociétés, Pratiques et Environnements, AASPE UMR 7209, CNRS/Muséum national d'Histoire naturelle, Paris, France
[b] Mécanismes adaptatifs et évolution, MECADEV UMR 7179, CNRS/ Muséum national d'Histoire naturelle, Paris, France
[c] Archéorient, Environnements et sociétés de l'orient ancien, UMR 5133, CNRS/Université de Lyon 2, Lyon, France
[d] Department of Archaeology, Lebanese University, Lebanon
[e] Microbial, Cellular and Molecular Biology, Addis Ababa University, Addis Ababa, Ethiopia
[f] Royal Belgian Institute of Natural Sciences, Brussels, Belgium
[g] CERMEP Imagerie du Vivant, Bron, France
[h] University of Tehran, Central Laboratory, Bioarchaeology Laboratory, Archaeozoology Section, Engelab av. Qods av., Poursina av., Jalalieh str. N° 6, CP1417634934 Tehran, Iran
[i] Université Côte d'Azur, CNRS, CEPAM (UMR 7264), Nice, France
[j] LiveGene, International Livestock Research Institute (ILRI), P.O. 5689, Addis Ababa, Ethiopia
[k] Amhara Regional Agricultural Research Institute, Bahir Dar, Ethiopia
[l] School of Life Sciences, University of Nottingham, University Park, Nottingham NG7 2RD, United Kingdom

ARTICLE INFO

Keywords:
Zooarchaeology
Bones morphometrics
Domestication
3D imaging

ABSTRACT

Over the last decade, the petrous bone (*petrosum*) has become the ultimate repository of ancient biomolecules, leading to a plea for a more ethical curation preventing the systematic destruction of this bioarchaeological archive. Here, we propose to explore the biosystematic signal encompassed in the biological form of 152 *petrosa* from modern populations of wild and domestic sheep landraces/breeds across Western Europe, South-Western Asia and Africa, using high resolution geometric morphometrics (GMM) and the latest development in 3D virtual morphology. We assessed the taxonomic signals among wild and domestic caprine species and sheep landraces. We also explored the effect of sexual dimorphism and ageing at the population scale. Finally, we assessed the influence of climatic factors across the geographic distribution of our dataset using Köppen-Geiger climate categories.

We found that the 3D form of petrous bones can accurately separate wild and domestic caprine taxa and that it is not influenced by sexual dimorphism, post-natal ageing or horn bearing. Recent selective breeding has not induced sufficient diversification to allow accurate identification of the different landraces/breeds in sheep; however, both genetic distance and climatic differences across the current distribution in sheep landraces/breeds strongly contribute to *petrosum* intraspecific variation. Finally, human mediated dispersal of domestic sheep outside their Near Eastern cradle, especially towards Africa, have greatly contributed to the diversification of sheep petrous bone form and shape. We therefore highly recommend systematic 3D surface modelling of archaeological *petrosa* with preliminary GMM studies to help target and reduce destructive biomolecular studies.

* Corresponding author.
E-mail address: cucchi@mnhn.fr (T. Cucchi).

https://doi.org/10.1016/j.jasrep.2022.103447
Received 21 November 2021; Received in revised form 11 March 2022; Accepted 7 April 2022

1. Introduction

The petrous bone (*petrosum*) forms part of the temporal bone and is located at the base of the endocranium, embedded in both the right and left temporal bones. It contains the organs for hearing and balance that constitute the bony labyrinth (the vestibule, the semi-circular canals and the cochlea). Along with teeth, the *petrosum* is one of the densest bones in the skeleton (Lam et al., 1999). It fully develops in utero without any remodelling throughout life (Mennecart and Costeur, 2016). Both these characteristics make it the ultimate repository of ancient biomolecules and endogenous ancient DNA in particular (Hansen et al., 2017; Kontopoulos et al., 2019; Pinhasi et al., 2015). Over the last few years, this has led to a rush in researchers accessing human and non-human mammalian archaeological petrous bones for biomolecular studies (Makarewicz et al., 2017). However, the extending demand for destructive analysis of these ancient remains (Fox and Hawks, 2019) has led to recent pleas for greater caution in the sampling strategy (Charlton et al., 2019) and a more ethical curation to safeguard these precious bioarchaeological archives (Pálsdóttir et al., 2019). Within the framework of the EvoSheep research project (Vila et al., 2021), which explores the history of sheep breeds in South-Western Asia (SWA), palaeogenetic studies have been performed on *petrosa* to extract endogenous DNA. These data are then used to reconstruct the selective breeding history of sheep – inducing the diversification and emergence of breeds adapted to various environments and needs – across the Fertile Crescent during the last 11,000 years. Before destructive sampling for DNA analysis is carried out, 3D surface scanning of archaeological petrous bones is performed, safeguarding a virtual image of each *petrosum* as an archive of the morphological variation in past populations of sheep. This study, therefore, provides an opportunity to assess the potential of the *petrosum* as a source of information on the diversity and evolution of ancient sheep populations following previous investigations on the astragalus (Colominas et al., 2019, Haruda et al., 2019, Pöllath et al 2019).

It is well known that variations in human and non-human mammalian skeletons result from both population history and local adaptation. However, heritable variations are difficult to decipher from non-heritable ones due to ecophenotypic plasticity (Caumul and Polly, 2005; von Cramon-Taubadel, 2011; von Cramon-Taubadel and Smith, 2012). The temporal bone and inner structures of the *petrosum* have been studied to track phylogenetic relationships among early hominids (Braga et al., 2017) and modern human populations (Urciuoli et al., 2021), as well as their dispersal out of Africa (de León et al., 2018; Smith et al., 2007). Physical anthropology has also explored the potential of the *petrosum* for sexing skulls, based on the angle of the internal auditory canal (Norén et al., 2005) and for estimating foetal age at death (Nagaoka, 2015). The use of the *petrosum* as a biosystematics marker has, however, been far less explored in the field of zooarchaeology. Their greater preservation compared to the rest of the cranial elements is a means to obtain a reliable estimate of cranial occurrences and therefore assess bone destruction and selective transport in faunal assemblages (Bar-Oz and Dayan, 2007). It has also been used to obtain morphoscopic identification at species level (Bar-Oz et al., 2019; O'leary, 2010), even for closely related species like sheep and goats, using multivariate morphometrics (Mallet et al., 2019; Mallet and Guadelli, 2013). However, despite a recent study on the inner ear variation in *Sus scrofa* (Evin et al., 2022), the intraspecific component of the petrous bones morphological variation has yet to be explored. Can it capture population and dispersal history? How much its development is impacted by sexual dimorphism or growth? How much can geoclimatic differences (elevation and climate) influence its morphological variation? If such signals could be captured from the variation in the morphology of the *petrosum*, they would prove useful for many studies dealing with the reconstruction of the origins and dispersal of domestic species, as well as facilitating targeted molecular destructive analyses as required by curators and stakeholders (Pálsdóttir et al., 2019).

In order to explore the biosystematic signals in the *petrosum*, we relied on a cross sectional study of skulls from modern populations of domestic sheep breeds and landraces across Western Europe, SWA and Africa, including wild sheep and domestic goats (Fig. 1). We relied on the known life history and the presence or absence of horns for each specimen to assess the influence of sexual dimorphism, age and horns bearing on morphological variation. Finally, altitudinal records and climatic categories for each population sample were used to assess the abiotic factors of variation in the petrous bone at an intraspecific scale. To prevent damage to the skull, we extracted a 3D virtual image of the petrous bone from the endocranium (Fig. 2A) using computerized tomography (CT) scanning. Its complex morphology was quantified with a 3D geometric morphometric (GMM) approach to separately explore its size, shape and form (size + shape) components. Thanks to the latest development in virtual morphology, this study provides options to reduce destructive sampling strategies and a means of keeping a virtual record of the bone after destruction for further biomolecular studies.

2. Material and methods

2.1. Material

We collected 132 domestic sheep skulls (*Ovis aries*) from 16 current breeds and landraces across SWA, Africa and Western Europe. We also collected the skulls of 12 wild sheep/mouflon (*Ovis aries musimon*) from Corsica and 4 wild sheep/mouflon (*Ovis orientalis*) from Iran as a proxy of the ancestral wild phenotype. Corsican mouflon is a particular subspecies of sheep, originating from domestic sheep populations introduced to Corsica during the Neolithic that have returned to the wild (Poplin, 1979; Vigne, 1992), not to be confused with "real" mouflon (*Ovis orientalis*), from which all the domestic breeds stem (Hiendleder et al., 2002). We also sampled four goats (*Capra hircus*) from France as a closely related species (Table 1; Fig. 1; Supplementary table 1 for a detailed list of the material). Sheep specimens lacking breeding information were grouped according to their geographic location and considered as landraces (i.e., Vaucluse, Alpes Maritimes, Ağlasun). For most of the specimens, the sex and age were known.

Collections from Dahomey (OA_DHO), Vaucluse (OA_VAU) and Gumz (OA_GUM), provided an ontogenetic series with ages ranging from juvenile to mature. For each specimen, phenotypic characteristic such as the presence and absence of horns and tail and coat types were registered and associated with a climatic category based on the Köppen-Geiger climate classification (Beck et al., 2018), estimated from each samples' origin. This classification is based on threshold values of seasonality, monthly air temperature and precipitation that can be used for species distribution modelling. In the same manner, each specimen was associated with one of four altitudinal groups ranging from 0 to 3000 m (See Tab. 1SI, Table 1).

2.2. 3D imaging

All skulls were CT scanned using the Siemens Magnetom Prisma 3 T scanner at the CERMEP Imagerie du vivant in Lyon, France. CT scan image stacks (DICOM format) were used to extract the 3D surfaces of the petrous bone using the "Isosurface'' module in Avizo™ 7.1 and 8.1 (FEI, France). We extracted the surface of the left petrous bone for all the specimens except 15 sheep whose left skull parts were not available. For those individuals, we created a mirror image of the right petrous bone using Avizo™ 8.1.

2.3. Geometric morphometrics

The protocol to capture the medial face of the *petrosum* has 237 3D Cartesian coordinates: 8 anatomical landmarks, 48 curve semilandmarks and 181 surface semilandmarks (Fig. 2B). Landmarks and semilandmarks were digitized using IDAV Landmark™ (UC Davis, USA). The 3D surface of the petrous bone was captured following published

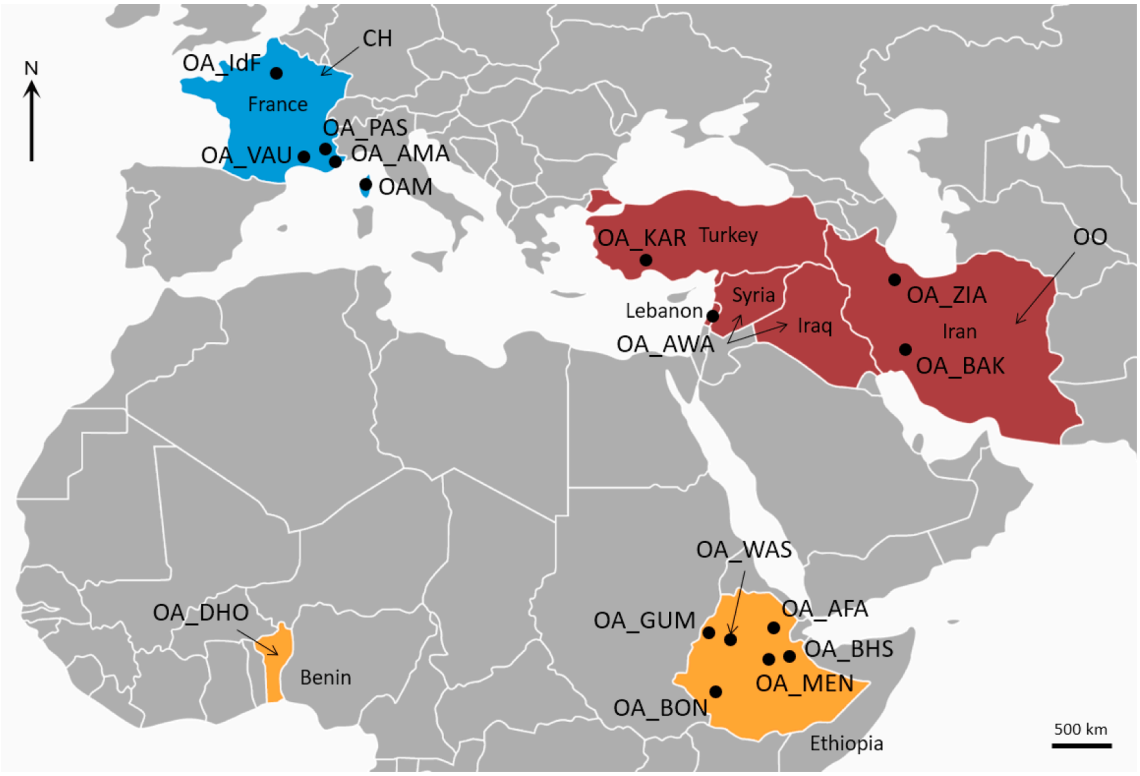

Fig. 1. Location of the different sheep breeds and landraces from South-Western Asia (Red), Africa (Orange) and Europe (Blue) used in this study. Black points indicate known locations. See Table 1 for grouping codes.

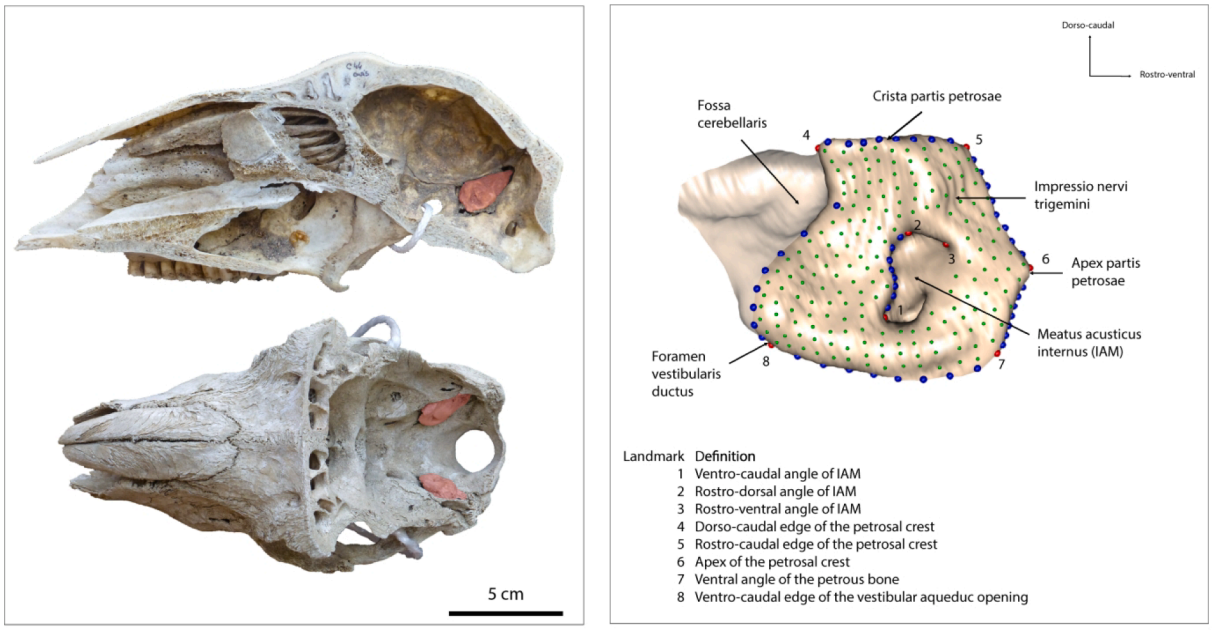

Fig. 2. A. Location of the *petrosum* (in red) within the sheep's endocranium. B. Anatomy of a left side petrous bone and its 3D GMM protocol.

protocols (Botton-Divet et al., 2016). Surface semilandmarks were manually placed on a template from a single specimen selected beforehand for its mean conformation with the 'findMeanSpec' function of the geomorph package (version 3.0.7; Adams and Otárola-Castillo, 2013) of R (R Core Team. 2020, version 4.0.2; RStudio Team. 2020, version 1.3.959-1).

This template was then used to project the semilandmarks onto the surface of the other specimens of the dataset using the 'placePatch' function of the Morpho package (version 2.6; Schlager, 2017). Projection was followed by a relaxation step to ensure that the projected points matched the actual surface of the mesh. The curve and surface semilandmarks were slid using the minimizing bending energy algorithm (Bookstein, 1998). The landmarks and semilandmarks could therefore be treated as geometrically homologous from one petrous bone to the next.

Finally, all the specimens were superimposed using a Generalized

Table 1
Summary table of the samples studied providing taxonomic, geographic, climatic, altitudinal and sample size information (full description per specimen is available in SI table 1). Climatic information has been defined after the Köppen-Geiger climate classification (Beck et al., 2018): Csa = Warm temperate climate/Dry_hot summer, Csb = Warm temperate climate/Dry_warm summer, Dsb = Snow/Dry_warm summer, BSk = Arid climate/Steppe_cold, BSh = Arid climate/Steppe_hot, Aw = Equatorial climate/Dry winter, Cfb = Warm temperate climate/Fully humid_warm summer, wa = Warm temperate climate/Winter dry_hot summer, Cwb = Warm temperate climate/Winter dry_warm summer. NA: not available.

Species / subspecies	Breed/ population	Tail	Coat	Geographic origin	Köppen-Geiger climate classification	Elevation (m)	Grouping code	Sample size
Capra hircus	Domestic Goat	Short tail	Hair	France	NA	NA	CH	4
Ovis orientalis	Mouflon	Short tail	Hair	Iran	BSk	2000–3000	OO	4
O. aries musimon	Corsican mouflon	Short tail	Hair	France	Csa	1000–2000	OAM	12
Ovis aries	Préalpes du Sud	Thin tail	Wool	France	Csb	500–1000	OA_PAS	6
Ovis aries	Île-de-France	Thin tail	Wool	France	Cfb	0–500	OA_IDF	2
Ovis aries	Alpes Maritimes	Thin tail	Wool	France	Csb	500–1000	OA_AMA	4
Ovis aries	Vaucluse	Thin tail	Wool	France	Csa	0–500	OA_VAU	13
Ovis aries	Ağlasun	Fat tail	Coarser wool	Turkey	Csa	1000–2000	OA_KAR	23
Ovis aries	Awassi	Fat tail	Coarser wool	Syria, Iraq, Lebanon	Csa	0–500	OA_AWA	18
Ovis aries	Ziaran	Fat tail	Coarser wool	Iran	Dsb	1000–2000	OA_ZIA	9
Ovis aries	Bakhtiari	Fat tail	Coarser wool	Iran	BSk	2000–3000	OA_BAK	13
Ovis aries	Dahomey	Thin tail?	Hair?	Benin	Aw	0–500	OA_DHO	7
Ovis aries	Bonga	Long fat tail	Hair	Ethiopia	Cfb	1000–2000	OA_BON	10
Ovis aries	Menz	Fat tail	Coarser wool	Ethiopia	Cwb	2000–3000	OA_MEN	4
Ovis aries	Washera	Fat tail	Hair	Ethiopia	Cwa	2000–3000	OA_WAS	5
Ovis aries	Gumz	Long thin tail	Hair	Ethiopia	Aw	500–1000	OA_GUM	9
Ovis aries	Black Head Somali	Fat rump	Hair	Ethiopia	BSh	500–1000	OA_BHS	4
Ovis aries	Afar	Fat rump	Hair	Ethiopia	BSh	500–1000	OA_AFA	5

Procrustes Analysis (GPA) (Bookstein, 1991; Rohlf and Slice, 1990) to remove the effects of position, orientation and size, along with an alignment procedure (translation, rotation, isotropic rescaling) to produce centroid size (size of geometric scale computed as the square root of the summed squared distances of each landmarks and the centroid of the landmarks configuration) and Procrustes coordinates for the size and shape components of the petrous bones' form. To obtain the 'form space' or 'size-shape space' of the petrous bones we augmented the Procrustes coordinates with the natural logarithm of the centroid size (Mitteroecker et al., 2004; Mitteroecker and Bookstein, 2011; Mitteroecker and Gunz, 2009).

The landmark digitization error was assessed by five repeated recordings of the anatomical landmarks and curves on five sheep specimens analysed by a Principal Component Analysis (PCA). All repeated measurements produced five well-separated clusters on the first two PCs, proving that measurement error did not interfere with biological differentiation among the five specimens.

GMM procedures were performed with the 'geomorph' (version 3.0.7) functions and the 'Morpho' (version 2.6) packages of R software (3.5.1, R Core Team).

2.4. Statistics

Size differences between individuals were tested with an Analysis of Variance (ANOVA) associated with pairwise comparisons (Collyer et al., 2015), on the whole dataset and on adult individuals above 12 months only.

Size variations among populations were visualized with boxplots for log-transformed centroid size. To test size differences between species and breeds/landraces, while considering sexual dimorphism and the presence or absence of horns, we used a factorial ANOVA.

Allometric changes (Klingenberg, 2016) and other covariations of the petrous bone shape or form with factors such as taxonomic differences (species breeds/landraces), sexual dimorphism (male vs. female), presence/absence of horns or climatic classification, and continuous variables such as age at death (ontogeny) or the elevation range of the population samples were tested with a Procrustes ANOVA and permutation procedures using the ProcD.lm function in 'geomorph' library (Adams and Otárola-Castillo, 2013) which takes into account both discrete and continuous type of factors. The Procrustes ANOVA to test the effect of sexual dimorphism was performed on samples with balanced males and females ratio such as Awassi, Bonga, Dahomey and Préalpes du Sud.

Patterns of shape and form differentiation among wild and domestic caprines (domestic sheep, wild sheep and domestic goat) were visualized with a between-group PCA (bgPCA) using the 'Morpho' library. To make sure that differenciation patterns of the bgPCA are not spurious (Cardini and Polly, 2020; Bookstein 2019) we have performed randomised tests (1000 repetitions) and cross validation using *ade4* package (Dray and Dufour 2007) following recommendations by Thioulouse et al. (2021). To observe intraspecific patterns of shape and form differentiation we used Canonical Variate Analysis (CVA) to maximize intergroup difference while minimizing intragroup variance. However, CVA can lead to spurious groupings when the number of variables exceed the number of individuals (Mitteroecker & Bookstein 2011, Kovarovic et al. 2011). To overcome this issue, we used the *Morpho* R package which implement the required data dimensionality reduction. To display shape deformations between the wild and domestic taxa we superimposed the warped shapes of each individual onto an average shape, selected beforehand by visually assessing which specimen was the most central in the PCA using the 'geomorph' library. Mean forms were obtained by adding the size component to the mean shapes. To visualize patterns of shape and form similarities and dissimilarities among samples we used a Neighbour-Joining tree on the Euclidean distances between the samples' mean shapes and forms computed from their PCA scores using the 'ape' library.

To assess the taxonomic resolution of *petrosum* shape and form variation at the interspecific and intraspecific levels, we used the k-Nearest-Neighbour (k-NN) algorithm (Ripley, 2007; Venables and Ripley, 2002) in the 'class' library. This nonparametric method consists of

classifying an object into a predefined group according to its Euclidean distance with its k-NN (k being a natural number). We tested with k ranging from 1 to n-1, n being the smallest number of individuals within a group, then calculated the mean of the values obtained. The k-NN predictions were performed between wild and domestic caprine (152 specimens), between wild and domestic sheep (132 specimens) and between sheep breeds/landraces (130 specimens; excluding breeds comprising less than 3 individuals).

All statistical analyses were performed in R using the R package 'MASS' (version 7.5-50; Venables and Ripley, 2002), 'picante' (version 1.8; Kembell et al., 2010) and 'class' (version 7.3-15; Venables and Ripley, 2002) in addition to the previously cited packages.

Data and R script are available at NAKALA. https://nakala.fr/https://doi.org/10.34847/nkl.3f58q69y.

3. Results

3.1. Petrous bone size, shape and form variation in wild and domestic caprines

Centroid size between *O. aries, O. aries musimon, O. orientalis* and *C. hircus* differed significantly ($p = 0.001$, $R^2 = 0.49$) (Fig. 3). Domestic goats have the largest petrous bones of all the caprine taxa in our dataset, even larger than wild sheep. Within the *Ovis* genus, domestic sheep have smaller petrous bones than their wild relative *O. orientalis*, with Corsican mouflons having an intermediate size.

The differences between domestic goat, domestic sheep and wild sheep are significant but small in petrous bone shape ($p = 0.001$, $R^2 = 0.05$) and much greater in form ($p = 0.001$, $R^2 = 0.19$).

Patterns of petrous bone shape differentiation among the four caprine taxa are significant (*randtest p-value* = 0.001). The bgPCA show that goat *petrosa* have a very different shape (Fig. 4) compared to those of wild and domestic sheep: the opening of the internal acoustic meatus (IAM) appears smaller and elongated along the rostro-caudal axis in goats, while the petrosal crest is thickened and forms a protuberance from the dorso-caudal extremity to the trigeminal nerve impression (Fig. 4). The most obvious differences between wild/feral and domestic sheep are the protuberance on the rostral part of the petrosal crest and a slightly more marked trigeminal impression. The domestic sheep and Corsican mouflon mean shapes are extremely similar; the only apparent

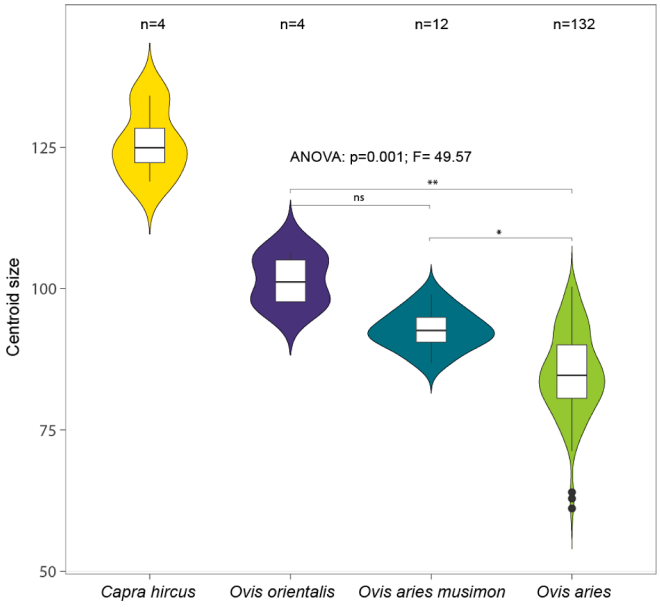

Fig. 3. Petrous bone Centroid size variation among wild, feral and domestic caprine species.

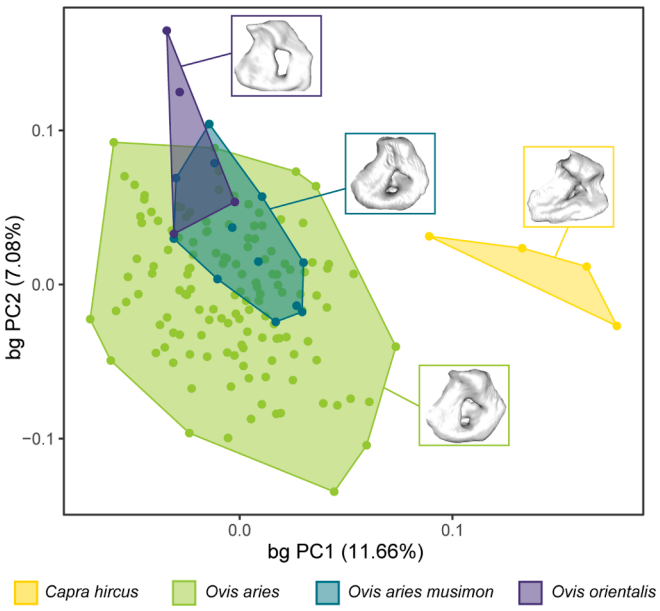

Fig. 4. BGPCA displaying the petrous bone mean shape among wild, feral and domestic sheep and domestic goats with the visualization of the petrous bone mean shape for each taxon.

differences being the wider rostro-ventral angle of the IAM and a slightly more convex petrosal crest in the latter. Ventro-caudal extremity is also flatter in the Corsican mouflon, resulting in a slightly less rounded shape.

The shape of the mouflon (*O. orientalis*) *petrosa* bears some distinct features: the concave angle of the dorsal edge is more marked than in Corsican mouflon and domestic sheep, and the IAM opening appears narrower and more angled along the dorso-caudal axis than it does in the other *Ovis* species.

3.2. Petrous bone size variation in wild and domestic sheep

The difference among landraces/breeds explains a very important part of the centroid size variation in sheep petrous bones ($p = 0.001$, $R^2 = 0.5$), although no clear geographic structuring of the variation was observed (Fig. 5). Removing the Iranian and Corsican mouflon, which are larger in size than all the other *Ovis* samples, three size groups ($p = 0.001$, $R^2 = 0.45$) can be observed: (1) a large one which includes three sheep samples from SWA (Bakhtiari and Awassi) and Africa (Gumz) in addition to the Corsican mouflon, (2) an intermediate one which includes all the French breeds, three African landraces (Washera, BHS, Bonga) and two SWA breeds (Ziaran and Käragoz) and (3) a small one which includes small African breeds (Afar and Menz) and the Dahomey sheep (DOH), which has the smallest petrous bone of all the sheep samples (see pairwise comparison in SI, Table 2).

3.3. Allometric influence over petrous bone shape variation in wild and domestic caprines

The allometry represents 3.8% of the variation among the four caprine taxa ($p = 0.001$) and 3.6% in domestic sheep. Allometric trajectories are shared across the wild and domestic caprine taxa (interaction term: $p = 0.19$) and the domestic sheep populations ($p = 0.49$). However, the common allometry is lost within domestic sheep breeds/landraces populations. Allometry, therefore, does not interfere with species differentiation but can interfere with breeds/landraces/populations in sheep.

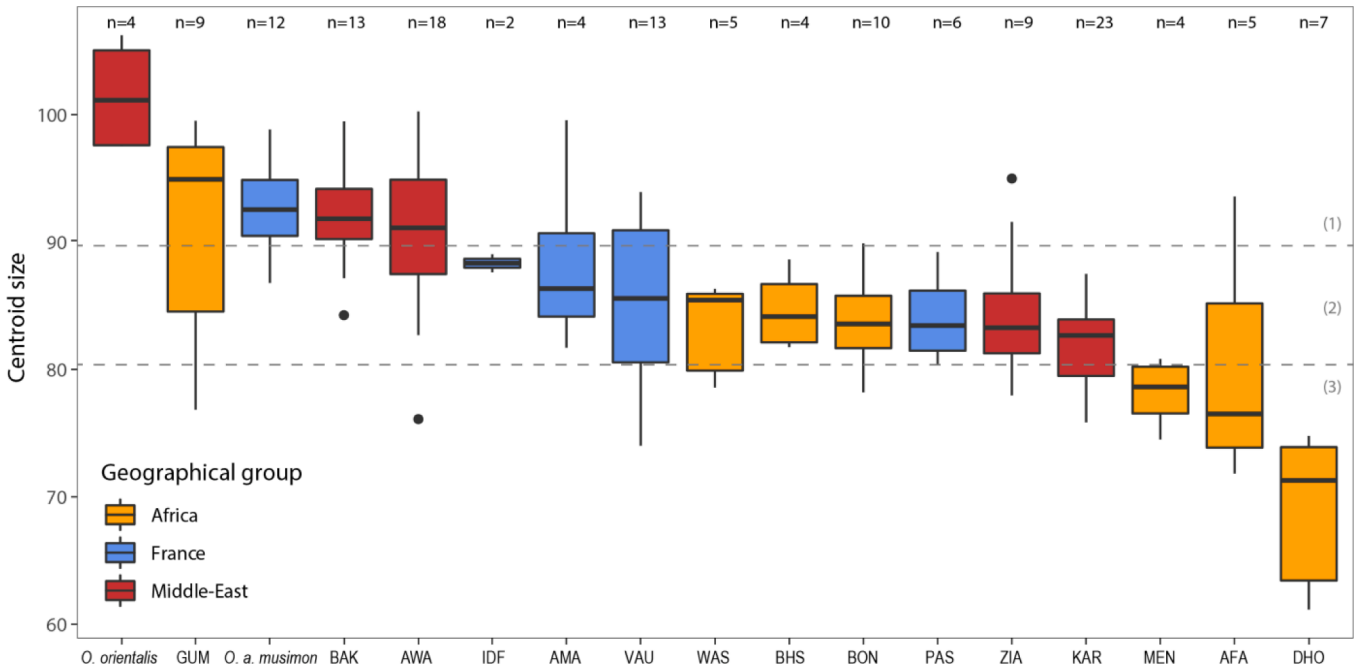

Fig. 5. Petrous bone centroid size in wild and domestic *Ovis* populations subdivided into three variation groups.

Table 2
Procrustes ANOVA testing for the covariation between petrous bone size, shape and form and Köpper-Geiger climatic classification (Climate) and altitudinal records for the samples (Elevation) among wild and domestic sheep species (*Ovis* spp.) and sheep breeds/landraces (*Ovis aries*).

	Climate			Elevation		
	Csize	Shape	Form	Csize	Shape	Form
Ovis sp.	**$p = 0.001$; $R^2 = 0.19$**	**$p = 0.001$; $R^2 = 0.14$**	**$p = 0.001$; $R^2 = 0.16$**	**$p = 0.027$; $R^2 = 0.06$**	$p = 0.08$; $R^2 = 0.03$	**$p = 0.02$; $R^2 = 0.04$**
Ovis aries	**$p = 0.01$; $R^2 = 0.13$**	**$p = 0.001$; $R^2 = 0.14$**	**$p = 0.001$; $R^2 = 0.14$**	$p = 0.19$; $R^2 = 0.03$	$p = 0.17$; $R^2 = 0.02$	$p = 0.12$; $R^2 = 0.03$

3.4. Influences of age, sex and horn bearing over petrous bone size and shape variation in Ovis

The age effect was significant on the size ($p = 0.002$, $R^2 = 0.36$) but not the shape ($p = 0.07$, $R^2 = 0.19$) variation of the petrous bone when taking all specimens into account; the effect was not present when removing juvenile (less than12 months) specimens ($p = 0.18$, $R^2 = 0.17$). We found a significant difference in shape which suggested a morphological difference between horned and polled sheep ($p = 0.03$, $R^2 = 0.01$); however, this difference was not found ($p = 0.17$, $R^2 = 0.01$) when we removed the wild sheep. Horn bearing had no observed effect on the petrous bone size variation ($p = 0.45$; $R^2 = 0.004$) or on the form ($p = 0.24$, $R^2 = 0.01$) of wild and domestic sheep petrous bones.

There was no sexual dimorphism in the petrous bone centroid size ($p = 0.66$, $R^2 = 0.006$), shape ($p = 0.6$, $R^2 = 0.03$) or form ($p = 0.79$, $R^2 = 0.02$).

3.5. Influence of geo-climatic factors over petrous bone size and shape variation in wild and domestic sheep

Climatic differences in sample distribution explains between 13% and 19% of the size, form and shape variation of the petrous bones in both wild and domestic *Ovis* species, as well as in domestic sheep breeds/landraces (Table 2). Altitudinal influence on the petrous bone morphological variation is very low with only a slight covariation with the *petrosum* size and form among the wild and domestic sheep species, though not among the sheep breeds/landraces.

3.6. Inter and intraspecific taxonomic signals in petrous bones form and shape

The k-NN algorithm (Fig. 6) reached 86.4% of correct classification when predicting the four wild and domestic caprine taxa and up to 86.2% when predicting the three wild and domestic sheep taxa. However, correct classification dropped to a 1:2 ratio when predicting sheep breeds and landraces. At the interspecific level, form and shape data provided similar results, but there is a large disparity at the intraspecific level where the form data allows twice the correct classification rate of the shape data to be obtained.

3.7. Form and shape differences and relationships among wild and domestic sheep

The difference between sheep breeds and landraces explains 23% and 34%, respectively, of the shape and form variation of their petrous bones (MANOVA shape: $p = 0.001$, $R^2 = 0.23$; form: $p = 0.001$, $R^2 = 0.34$). Data using only curves exhibited the same differences but with reduced coefficient of variation R^2 (shape: $p = 0.001$, $R^2 = 0.22$; form: $p = 0.001$, $R^2 = 0.29$).

Both patterns of shape and form similarities and dissimilarities among wild, feral and domestic sheep populations (Fig. 7) were structured according to the divergence between African breeds and Eurasian wild sheep, domestic breeds and landraces. Within the Eurasian cluster, we observed a mixture between the European and SWA breeds, suggesting a lack of isolation by distance (IBD) phenomenon.

Within this Eurasian diversity, the wild populations (*O. orientalis, O. a.musimon*) clustered with the Near Eastern Awassi (OA_AWA) and

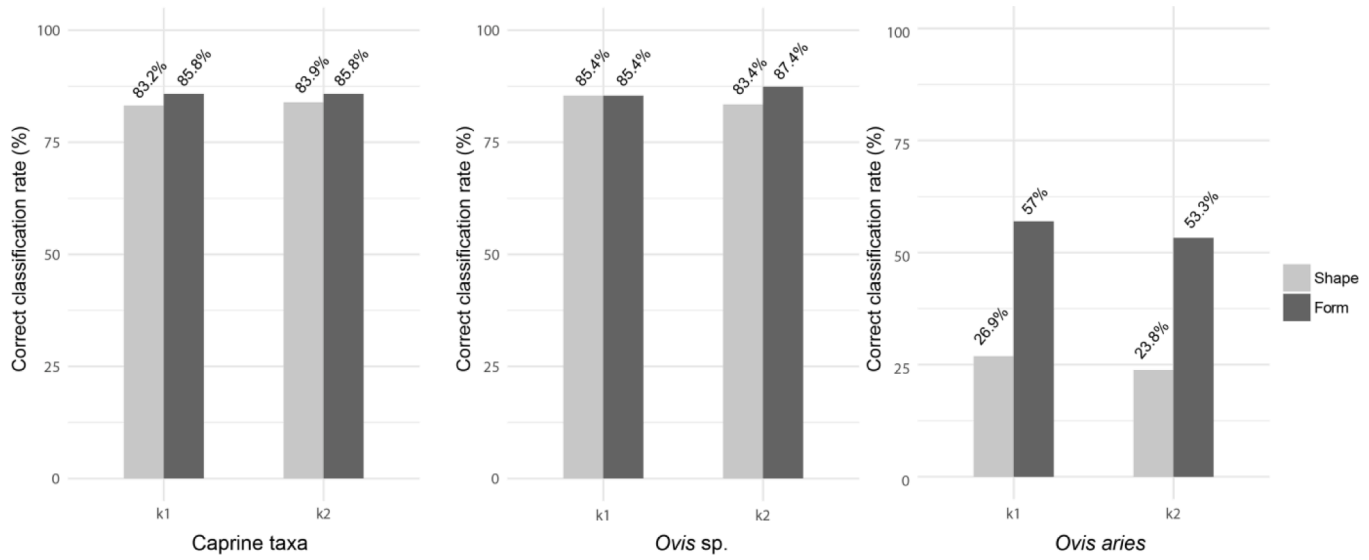

Fig. 6. Percentage of correct k-NN predictions of caprine species (Caprine taxa), wild and domestic sheep species (*Ovis* sp.) and sheep breeds/landraces *(Ovis aries)* using the petrous bone shape and form variations.

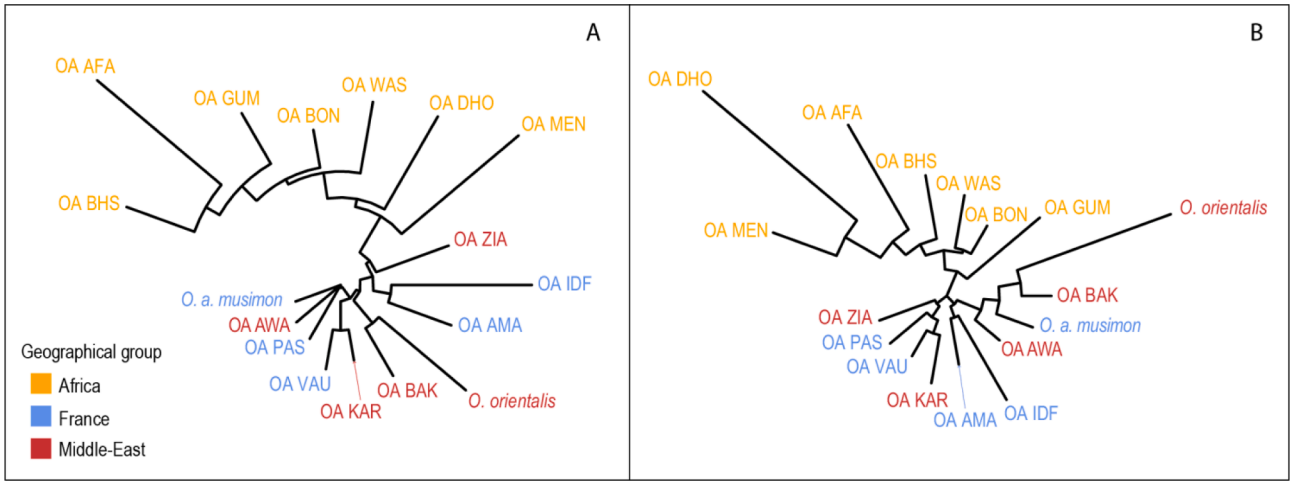

Fig. 7. Patterns of shape (A) and form (B) relationships in modern wild and domestic sheep using a Neighbour-joining tree computed on Euclidean distances between species/population mean.

Iranian Bakhtiari (OA_BAK) breeds. In SWA breeds, we also noticed a similarity in shape and form between the Ziaran and Karagöz populations (See also CVA in SI Fig. 1), respectively from Northern Iran and Anatolia. Among the European breeds (See also CVA in SI Fig, 2), both shape and form found a phenotypic similarity between the French breeds of Vaucluse (OA_VAU), the Préalpes du Sud (OA_PAS) and the Anatolian Karagöz (OA_KAR). This intricate structure may be linked to the geographic origin of sheep domestication in the Fertile Crescent. The Iranian Ziaran population (OA_ZIA) displayed the greatest phenotypic similarity with African diversity.

The African morphogroup showed greater diversity and strong divergence from their ancestral wild relative *O. orientalis*. We noticed a divergence of the Dahomey breed (OA_DHO) from the Ethiopian breeds (See also CVA in SI Fig. 3). Within the Ethiopian breeds, the Afar and BHS breeds are most closely related.

4. Discussion

For this study, we collected the virtual morphology of 152 petrous bones from the skulls of modern wild, feral and domestic caprines spread from across SWA, Western Europe and Africa. We wanted to assess whether the morphological variation of this bone could distinguish sheep populations and facilitate sampling strategies for biomolecular studies, as well as hopefully reducing the destruction rate of this archaeological record. We designed a 3D GMM protocol to capture the complex topography of the petrous bone surface using CT scanning to prevent any damage of the osteological collections.

4.1. Interspecific taxonomic signal

The taxonomic resolution of the petrous bone clearly distinguishes the domestic goat (*Capra hircus)* from wild and domestic sheep, supporting previous results obtained from multivariate morphometrics (Mallet et al., 2019). The phenotype of the Corsican mouflon, intermediate between the domestic and SWA mouflon, supports recent GMM cranial studies on Australian feral boars descended from 19th century introduced pigs, showing that the feralization of a domestic population does not lead to the return of a wild phenotype (Neaux et al., 2020). However, the phenotype of the Corsican mouflon could also be related to an insular rather than a domestication syndrome, as shown for the now

extinct endemic wild boar of Cyprus introduced by Epipalaeolithic hunter-gatherers (Cucchi et al., 2021; Vigne et al., 2009).

4.2. Life-trait signals

At the intraspecific level, we found no differences between males and females in the size or form of the petrous bones and only a very slight effect on shape: This contradicts previous studies on modern humans (Wahl and Graw, 2001) but supports recent studies on horses (Clavel et al., 2021). This suggests that petrous bone morphological variation, at least in sheep and horses, has no resolution for the discrimination between males and females.

Concerning the influence of age on shape and form, the age after birth from juveniles to adults has no significant influence over the morphological variation of the petrous bone. Although age related change can be observed during the first weeks after birth in the mesial morphology of the caprine petrous bone (Mallet et al., 2019; Mallet and Guadelli, 2013), our results support another study which shows that beyond foetal age at death, petrous bone morphological variation is not influenced by post-natal growth (Nagaoka and Kawakubo, 2015); therefore, the admixture of petrous bones from juvenile and adults in the archaeological record does not interfere in their taxonomic resolution.

While one fifth of the skulls belonged to horned animals, we found no influence due to the presence or absence of horns on the shape and form of the petrous bone. This could suggest that the long-lasting husbandry practice for selecting hornless sheep, despite its strong signature in the genome (Kijas et al., 2012), has not impacted petrous bone morphological variation.

4.3. Genetic and climatic signals

We found a significant influence from both genetic and climatic factors in the variation of the petrous bone of wild and domestic sheep. Speciation and population history may explain a greater amount of the phenotypic variation of the *petrosum* than climatic difference across the distribution of sheep breeds and landraces, but the influence of the latter is far from being negligible. This result contradicts studies on modern humans showing that the cranial base morphology in general (Harvati and Weaver, 2006; Lieberman et al., 2000) and the temporal bone in particular (Smith et al., 2007) is mainly driven by genetic and geographic distances, according to the IBD model, and is relatively unaffected by environmental factors. The first potential reason for the discrepancy between our studies is that the statistical approach we implemented to test the covariation between morphology and climate used climatic categories with multivariate regression models and not climatic variables with the matrix correlation or Partial Least Square (PLS) approaches used in modern human studies. The other reason is that selective pressures of climate in the evolutionary history of modern humans cannot be fully compared with the population history of wild and domestic sheep. Most of the *Ovis aries* populations from our dataset are traditional breeds/landraces that have been locally adapted to their natural and cultural environment through anthropogenic selection and some sort of genetic isolation during the domestication process (Kijas et al., 2012).

4.4. Selective breeding and population history

An accurate discrimination of the different *Ovis aries* breeds and landraces from our dataset has proved unattainable using the size and the shape of the petrous bones and only to a limited extent with form. Despite using a GMM approach, it is still difficult to access predictive identification at the intraspecific level, as has already been shown for a horse's bony labyrinth (Clavel et al., 2021) and bovine teeth (Cucchi et al., 2019). It is possible that intraspecific differences are best seen in populations that have been subjected to significant genetic isolation and selective pressure, as observed between two equine breeds (Seetah et al., 2014). Indeed, our results clearly show that the petrous bone form and shape variation has encapsulated deep anthropogenic sheep phylogeography, such as the spread of sheep from the Near East to Africa through several dispersal waves over time with Ethiopia as a gateway (Gizaw et al., 2007; Muigai and Hanotte, 2013). We found that all the African breeds represent a divergent morphogroup from their ancestral relative in SWA with the Dahomey sheep showing the greatest divergence. This landrace could be the Fouta-Djallon, a thin-tailed hairy breed described in 1950 (Anonymous, 1950). Within the African diversity, we found a differentiation pattern between the Afar and BHS fat rump breeds from arid climates, considered as the latest dispersal through the Arabian Peninsula and Yemen, and the western breed (Gumz), a thin-tailed breed, considered as an early arrival through Sudan. These results strongly suggest that the successive dispersal waves have left an imprint in the petrous bone morphological variation through the IBD model. Finally, the petrosal form proximity between European and Middle Eastern sheep populations agrees with archaeological knowledge concerning the initial spread of domestic ungulates and genetic information from retrovirus integrations and phylogeographic patterns (Chessa et al., 2009; Kijas et al., 2012; Peters et al., 2013; Vigne, 2008). The proximity of two Near Eastern breeds (Awassi and Bakhtiari), that live in the geographic region of sheep initial domestication, with the oriental wild sheep on one side and the Corsican mouflon on the other, probably mirror these heredities and trajectories.

5. Conclusion

This study on 152 domestic and wild sheep from various localities in Eurasia and Africa has explored the biosystematics potential of the petrous bone in bioarchaeology. The distinction between sheep and goats is highly accurate, as is the distinction within *Ovis* sp. between SWA mouflons, Corsican mouflons and the domestic taxa taken as a whole. At the intraspecific level, we can provide strong evidence that sexual dimorphism, age variation or the presence or absence of horns did not contribute significantly to the variation of the petrous and therefore did not interfere with the taxonomic signals. However, the distinction accuracy among sheep landraces and breeds dropped to an unreliable threshold despite the significant influence of population history on the differentiation patterns. Increasing the sample size, especially for underrepresented populations, would surely improve the intraspecific resolution. Petrous bone variation has nonetheless recorded deep human mediated dispersal waves of domestic sheep outside their Near Eastern cradle and especially towards Africa. Further studies are now required to disentangle the respective roles of selective breeding and climatic adaptations. For all these reasons, we suggest that archaeological petrous bones, either isolated or still inserted in the temporal bone, should be digitized to produce 3D models. These models should be produced via photogrammetry, portable 3D structured light scanning or Computed-Tomography scanning, since all these methods yield similar image surface representation and shape variables (Waltenberger et al., 2021). Finally, the GMM study of these 3D models would facilitate targeted biomolecular sampling strategies and reduce the amount of destructive sampling of petrous bones. The curation of these 3D models would also safeguard potential future research studies.

Declaration of Competing Interest

The authors declare that they have no known competing financial interests or personal relationships that could have appeared to influence the work reported in this paper.

Acknowledgements

This work was funded by the French National Research Agency (EvoSheep- ANR-17-CE27-0004). Modern Osteological Collection preparation were funded by: Evosheep ANR for Lebanese Breed; the

CGIAR Livestock CRP and Evosheep ANR for Ethiopian Breeds; Fyssen Foundation for Iranian breeds. We specially thank the following people and institutions for their logistical help and support; in Lebanon: the General Direction of Antiquity, Lebanese University. In Ethiopia: Shanbel Besufkad and Derib Aydefruhim (Debre Birhan Agricultural Research Center); Adebabay Kebede (Bahir Dar Regional Animal Health Laboratory); Zinash Abedde Lemma (ARCCH, Addis Abeba); C. Ménard (CFEE Addis Abeba); Bonga Agricultural Research Center; Guba & Almeha office of Agriculture. In Iran: the Bioarchaeology Laboratory-Central Laboratory, University of Tehran. In France: L. Zimmer (CERMEP, Lyon); M. Keller (INRA/CNRS). Many thanks to Raphaël Cornette for his technical support with the GMM of the petrous bone.

Appendix A. Supplementary data

Supplementary data to this article can be found online at https://doi.org/10.1016/j.jasrep.2022.103447.

References

Adams, D.C., Otárola-Castillo, E., 2013. geomorph: an r package for the collection and analysis of geometric morphometric shape data. Methods Ecol. Evol. 4, 393–399. https://doi.org/10.1111/2041-210X.12035.

Anonymous, N.O., 1950. Les races ovines et caprines de l'Afrique occidentale française (conférence de Luknow, 13–22 février 1950). Revue d'Elevage et de Médecine Vétérinaire des Pays Tropicaux 4 (4), 193.

Bar-Oz, G., Dayan, T., 2007. FOCUS: on the use of the petrous bone for estimating cranial abundance in fossil assemblages. J. Archaeol. Sci. 34, 1356–1360. https://doi.org/10.1016/j.jas.2006.10.021.

Bar-Oz, G., Marom, N., Pinhasi, R., 2019. Taxonomic identification of petrosal bone morphology. Bioarchaeol. Near East 13, 15–21.

Beck, H.E., Zimmermann, N.E., McVicar, T.R., Vergopolan, N., Berg, A., Wood, E.F., 2018. Present and future Köppen-Geiger climate classification maps at 1-km resolution. Sci Data 5, 180214. https://doi.org/10.1038/sdata.2018.214.

Bookstein, F., 1998. Morphometric tools for landmark data: geometry and biology. Biometrics 54 (1), 398.

Bookstein, F.L., 1991. Morphometric tools for landmark data Cambridge University Press. New York.

Bookstein, F.L., 2019. Pathologies of between-groups principal components analysis in geometric morphometrics. Evol. Biol. 46, 271–302. https://doi.org/10.1007/s11692-019-09484-8.

Botton-Divet, L., Cornette, R., Fabre, A.-C., Herrel, A., Houssaye, A., 2016. Morphological analysis of long bones in semi-aquatic mustelids and their terrestrial relatives. Integr. Comp. Biol. 56, 1298–1309. https://doi.org/10.1093/icb/icw124.

Braga, J., Bouvier, P., Romeyer Dherbey, J., Balaresque, P., Risser, L., Loubes, J.-M., Dumoncel, J., Duployer, B., Tenailleau, C., 2017. Echoes from the past: New insights into the early hominin cochlea from a phylo-morphometric approach. Comptes Rendus Palevol, Hominin biomechanics, virtual anatomy and inner structural morphology: From head to toe. A tribute to Laurent Puymerail 16, 508–520. doi: 10.1016/j.crpv.2017.02.003.

Caumul, R., Polly, P.D., 2005. Phylogenetic and environmental components of morphological variation: skull, mandible, and molar shape in marmots (Marmota, Rodentia). Evolution 59 (11), 2460–2472.

Charlton, S., Booth, T., Barnes, I., 2019. The problem with petrous? A consideration of the potential biases in the utilization of pars petrosa for ancient DNA analysis. World Archaeol. 51, 574–585. https://doi.org/10.1080/00438243.2019.1694062.

Chessa, B., Pereira, F., Arnaud, F., Amorim, A., Goyache, F., Mainland, I., Kao, R.R., Pemberton, J.M., Beraldi, D., Stear, M.J., Alberti, A., Pittau, M., Iannuzzi, L., Banabazi, M.H., Kazwala, R.R., Zhang, Y.-P., Arranz, J.J., Ali, B.A., Wang, Z., Uzun, M., Dione, M.M., Olsaker, I., Holm, L.-E., Saarma, U., Ahmad, S., Marzanov, N., Eythorsdottir, E., Holland, M.J., Ajmone-Marsan, P., Bruford, M.W., Kantanen, J., Spencer, T.E., Palmarini, M., 2009. Revealing the history of sheep domestication using retrovirus integrations. Science 324, 532–536. https://doi.org/10.1126/science.1170587.

Clavel, P., Dumoncel, J., Der Sarkissian, C., Seguin-Orlando, A., Calvière-Tonasso, L., Schiavinato, S., Chauvey, L., Perdereau, A., Aury, J.-M., Wincker, P., Onar, V., Clavel, B., Lepetz, S., Braga, J., Orlando, L., 2021. Assessing the predictive taxonomic power of the bony labyrinth 3D shape in horses, donkeys and their F1-hybrids. J. Archaeol. Sci. 131, 105383 https://doi.org/10.1016/j.jas.2021.105383.

Collyer, M.L., Sekora, D.J., Adams, D.C., 2015. A method for analysis of phenotypic change for phenotypes described by high-dimensional data. Heredity 115, 357–365. https://doi.org/10.1038/hdy.2014.75.

von Cramon-Taubadel, N., 2011. Global human mandibular variation reflects differences in agricultural and hunter-gatherer subsistence strategies. PNAS 108, 19546–19551. https://doi.org/10.1073/pnas.1113050108.

Colominas, L., Evin, A., Burch, J., Campmajó, P., Casas, J., Castanyer, P., Carreras, C., Guardia, J., Olesti, O., Pons, E., Tremoleda, J., Palet, J.-M., 2019. Behind the steps of ancient sheep mobility in Iberia: new insights from a geometric morphometric approach. Archaeol. Anthropol. Sci. 11, 4971–4982. https://doi.org/10.1007/s12520-019-00837-0.

Cucchi, T., Domont, A., Harbers, H., Evin, A., Alcàntara Fors, R., Saña, M., Leduc, C., Guidez, A., Bridault, A., Hongo, H., Price, M., Peters, J., Briois, F., Guilaine, J., Vigne, J.-D., 2021. Bones geometric morphometrics illustrate 10th millennium cal. BP domestication of autochthonous Cypriot wild boar (Sus scrofa circeus nov. ssp). Sci. Rep. 11 (1) https://doi.org/10.1038/s41598-021-90933-w.

Cucchi, T., Stopp, B., Schafberg, R., Lesur, J., Hassanin, A., Schibler, J., 2019. Taxonomic and phylogenetic signals in bovini cheek teeth: Towards new biosystematic markers to explore the history of wild and domestic cattle. J. Archaeol. Sci. 109, 104993.

Ponce de León, M.S., Koesbardiati, T., Weissmann, J.D., Milella, M., Reyna-Blanco, C.S., Suwa, G., Kondo, O., Malaspinas, A.-S., White, T.D., Zollikofer, C.P.E., 2018. Human bony labyrinth is an indicator of population history and dispersal from Africa. Proc. Natl. Acad. Sci. 115 (16), 4128–4133.

Dray, S., Dufour, A.B., 2007. The ade4 package: implementing the duality diagram for ecologists. J. Stat. Softw. 22, 1–20. https://doi.org/10.18637/jss.v022.i04.

Evin, Allowen, David, Loïc, Sauron, Antoine, Mennecart, Bastien, Orliac, Maeva, Lebrun, Renaud, et al., 2022. Size and shape of the semicircular canal of the inner ear: A new marker of pig domestication? Journal of Experimental Zoology Part B: Molecular and Developmental Evolution. https://doi.org/10.1002/jez.b.23127.

Fox, K., Hawks, J., 2019. Use ancient remains more wisely. Nature 572, 581–583. https://doi.org/10.1038/d41586-019-02516-5.

Gizaw, S., Arendonk, J.A.M.V., Komen, H., Windig, J.J., Hanotte, O., 2007. Population structure, genetic variation and morphological diversity in indigenous sheep of Ethiopia. Anim. Genet. 38, 621–628. https://doi.org/10.1111/j.1365-2052.2007.01659.x.

Hansen, H.B., Damgaard, P.B., Margaryan, A., Stenderup, J., Lynnerup, N., Willerslev, E., Allentoft, M.E., Caramelli, D., 2017. Comparing ancient DNA preservation in petrous bone and tooth cementum. PLoS ONE 12 (1), e0170940.

Haruda, A.F., Varfolomeev, V., Goriachev, A., Yermolayeva, A., Outram, A.K., 2019. A new zooarchaeological application for geometric morphometric methods: Distinguishing Ovis aries morphotypes to address connectivity and mobility of prehistoric Central Asian pastoralists. J. Archaeol. Sci. 107, 50–57. https://doi.org/10.1016/j.jas.2019.05.002.

Harvati, K., Weaver, T.D., 2006. Human cranial anatomy and the differential preservation of population history and climate signatures. The Anatomical Record Part A: Discoveries in Molecular, Cellular, and Evolutionary Biology 288A, 1225–1233. https://doi.org/10.1002/ar.a.20395.

Hiendleder, S., Kaupe, B., Wassmuth, R., Janke, A., 2002. Molecular analysis of wild and domestic sheep questions current nomenclature and provides evidence for domestication from two different subspecies. Proc. Biol. Sci. 269, 893–904. https://doi.org/10.1098/rspb.2002.1975.

Kijas, J.W., Lenstra, J.A., Hayes, B., Boitard, S., Porto Neto, L.R., San Cristobal, M., Servin, B., McCulloch, R., Whan, V., Gietzen, K., Paiva, S., Barendse, W., Ciani, E., Raadsma, H., McEwan, J., Dalrymple, B., Tyler-Smith, C., 2012. Genome-wide analysis of the world's sheep breeds reveals high levels of historic mixture and strong recent selection. PLoS Biol. 10 (2), e1001258.

Klingenberg, C.P., 2016. Size, shape, and form: concepts of allometry in geometric morphometrics. Dev. Genes. Evol. 226, 113–137. https://doi.org/10.1007/s00427-016-0539-2.

Kontopoulos, I., Penkman, K., McAllister, G.D., Lynnerup, N., Damgaard, P.B., Hansen, H.B., Allentoft, M.E., Collins, M.J., 2019. Petrous bone diagenesis: a multi-analytical approach. Palaeogeogr. Palaeoclimatol. Palaeoecol. 518, 143–154. https://doi.org/10.1016/j.palaeo.2019.01.005.

Kovarovic, K., Aiello, L.C., Cardini, A., Lockwood, C.A., 2011. Discriminant function analyses in archaeology: are classification rates too good to be true? J. Archaeol. Sci. 38 (11), 3006–3018.

Lam, Y.M., Chen, X., Pearson, O.M., 1999. Intertaxonomic variability in patterns of bone density and the differential representation of bovid, cervid, and equid elements in the archaeological record. Am. Antiq. 64, 343–362. https://doi.org/10.2307/2694283.

Lieberman, D.E., Ross, C.F., Ravosa, M.J., 2000. The primate cranial base: Ontogeny, function, and integration. Am. J. Phys. Anthropol. 113, 117–169. https://doi.org/10.1002/1096-8644(2000)43:31+<117::AID-AJPA5>3.0.CO;2-I.

Makarewicz, C., Marom, N., Bar-Oz, G., 2017. Ensure equal access to ancient DNA. Nature 548, 158. https://doi.org/10.1038/548158a.

Mallet, C., Cornette, R., Guadelli, J.-L., 2019. Morphometrical distinction between sheep (Ovis aries) and goat (Capra hircus) using the petrosal bone: application on French protohistoric sites. Int. J. Osteoarchaeology 29, 525–537.

Mallet, C., Guadelli, J.-L., 2013. Distinctive features of Ovis aries and Capra hircus petrosal parts of temporal bone: Applications of the features to the distinction of some other Caprinae (Capra ibex, Rupicapra rupicapra). PALEO. Revue d'archéologie préhistorique (24), 173–191.

Mennecart, B., Costeur, L., 2016. A Dorcatherium (Mammalia, Ruminantia, Middle Miocene) petrosal bone and the tragulid ear region. J. Vertebr. Paleontol. 36 (6), e1211665.

Mitteroecker, P., Bookstein, F., 2011. Linear discrimination, ordination, and the visualization of selection gradients in modern morphometrics. Evol. Biol. 38 (1), 100–114.

Mitteroecker, P., Gunz, P., 2009. Advances in geometric morphometrics. Evol. Biol. 36 (2), 235–247.

Mitteroecker, P., Gunz, P., Bernhard, M., Schaefer, K., Bookstein, F.L., 2004. Comparison of cranial ontogenetic trajectories among great apes and humans. J. Hum. Evol. 46 (6), 679–698.

Muigai, A.W.T., Hanotte, O., 2013. The origin of African sheep: archaeological and genetic perspectives. African Archaeol. Rev. 30 (1), 39–50.

Nagaoka, T., Kawakubo, Y., 2015. Using the petrous part of the temporal bone to estimate fetal age at death. Forensic Sci. Int. 248, 188.e1. https://doi.org/10.1016/j.forsciint.2015.01.009.

Neaux, D., Sansalone, G., Lecompte, F., Haruda, A., Schafberg, R., Cucchi, T., 2020. Examining the effect of feralization on craniomandibular morphology in pigs, Sus scrofa (Artiodactyla: Suidae). Biol. J. Linn. Soc. 131, 870–879. https://doi.org/10.1093/biolinnean/blaa156.

Norén, A., Lynnerup, N., Czarnetzki, A., Graw, M., 2005. Lateral angle: A method for sexing using the petrous bone. Am. J. Phys. Anthropol. 128, 318–323. https://doi.org/10.1002/ajpa.20245.

O'leary, M.A., 2010. An anatomical and phylogenetic study of the osteology of the petrosal of extant and extinct artiodactylans (Mammalia) and relatives. Bull. Am. Museum Natural History 2010, 1–206.

Pálsdóttir, A.H., Bläuer, A., Rannamäe, E., Boessenkool, S., Hallsson, J.H., 2019. Not a limitless resource: ethics and guidelines for destructive sampling of archaeofaunal remains. R. Soc. Open Sci. 6 (10), 191059.

Peters, J., Buitenhuis, H., Grupe, G., Schmidt, K., Pöllath, N., 2013. The Long and Winding Road: Ungulate Exploitation and Domestication in Early Neolithic Anatolia (10,000–7,000 cal BC). Left Coast Press, Walnut Creek, CA, 83-114.

Pinhasi, R., Fernandes, D., Sirak, K., Novak, M., Connell, S., Alpaslan-Roodenberg, S., Gerritsen, F., Moiseyev, V., Gromov, A., Raczky, P., Anders, A., Pietrusewsky, M., Rollefson, G., Jovanovic, M., Trinhhoang, H., Bar-Oz, G., Oxenham, M., Matsumura, H., Hofreiter, M., Petraglia, M.D., 2015. Optimal Ancient DNA Yields from the Inner Ear Part of the Human Petrous Bone. PLoS ONE 10 (6), e0129102.

Pöllath, N., Schafberg, R., Peters, J., 2019. Astragalar morphology: approaching the cultural trajectories of wild and domestic sheep applying Geometric Morphometrics. J. Archaeolog. Sci.: Rep. 23, 810–821. https://doi.org/10.1016/j.jasrep.2018.12.004.

Poplin, F., 1979. Origine du Mouflon de Corse dans une nouvelle perspective paléontologique: par marronnage, in: Annales de Génétique et de Sélection Animale. BioMed Central, p. 133.

R Core Team. 2020. R: A language and environment for statistical computing. R Foundation for Statistical Computing, Vienna, Austria. https://www.R-project.org/.

RStudio Team. 2020. RStudio: Integrated Development for R. RStudio, Inc., Boston, MA. http://www.rstudio.com/.

Ripley, B.D., 2007. Pattern recognition and neural networks. Cambridge university press.

Rohlf, F.J., Slice, D., 1990. Extensions of the Procrustes method for the optimal superimposition of landmarks. Syst. Biol. 39, 40–59.

Schlager, S., 2017. Chapter 9 – Morpho and Rvcg – Shape analysis in R: R-packages for geometric morphometrics, shape analysis and surface manipulations. In: Zheng, G., Li, S., Székely, G. (Eds.), Statistical Shape and Deformation Analysis. Academic Press, pp. 217–256. https://doi.org/10.1016/B978-0-12-810493-4.00011-0.

Seetah, K., Cucchi, T., Dobney, K., Barker, G., 2014. A geometric morphometric re-evaluation of the use of dental form to explore differences in horse (Equus caballus) populations and its potential zooarchaeological application. J. Archaeol. Sci. 41, 904–910. https://doi.org/10.1016/j.jas.2013.10.022.

Smith, H.F., Terhune, C.E., Lockwood, C.A., 2007. Genetic, geographic, and environmental correlates of human temporal bone variation. Am. J. Phys. Anthropol. 134, 312–322. https://doi.org/10.1002/ajpa.20671.

Thioulouse, J., Renaud, S., Dufour, A.-B., Dray, S., 2021. Overcoming the spurious groups problem in between-group PCA. Evol. Biol. 48 (4), 458–471.

Urciuoli, A., Zanolli, C., Almécija, S., Beaudet, A., Dumoncel, J., Morimoto, N., Nakatsukasa, M., Moyà-Solà, S., Begun, D.R., Alba, D.M., 2021. Reassessment of the phylogenetic relationships of the late Miocene apes Hispanopithecus and Rudapithecus based on vestibular morphology. Proc. Natl. Acad. Sci. U.S.A. 118 (5).

Venables, W.N., Ripley, B.D., 2002. Modern applied statistics (Fourth S., editor) New York. Springer.

Vigne, J.-D., 2008. Zooarchaeological aspects of the Neolithic diet transition in the Near East and Europe, and their putative relationships with the Neolithic demographic transition, in: The Neolithic Demographic Transition and Its Consequences. Springer, pp. 179–205.

Vigne, J.-D., 1992. Zooarchaeology and the biogeographical history of the mammals of Corsica and Sardinia since the last ice age. Mammal Review 22 (2), 87–96.

Vigne, J.-D., Zazzo, A., Saliège, J.-F., Poplin, F., Guilaine, J., Simmons, A., 2009. Pre-Neolithic wild boar management and introduction to Cyprus more than 11,400 years ago. PNAS 106, 16135–16138. https://doi.org/10.1073/pnas.0905015106.

Vila, E., Abrahami, P., Albesso, M., Amane, A., Bader, C., Berthon, R., Bouzid, S., Bradley, D., Breniquet, C., Chahoud, J., Cucchi, T., Davoudi, H., de Cupere, B., Escarguel, G., Estrada, O., Gourichon, L., Helmer, D., Huangfu, W., Lesur, J., Mashkour, M., Michel, C., Mohaseb, A., Orlando, L., Pompanon, F., Studer, J., Vuillien, M., 2021. EVOSHEEP: the makeup of sheep breeds in the ancient Near East. Antiquity 95, 379. https://doi.org/10.15184/aqy.2020.247.

von Cramon-Taubadel, N., Smith, H.F., 2012. The relative congruence of cranial and genetic estimates of hominoid taxon relationships: Implications for the reconstruction of hominin phylogeny. J. Hum. Evol. 62, 640–653. https://doi.org/10.1016/j.jhevol.2012.02.007.

Wahl, J., Graw, M., 2001. Metric sex differentiation of the pars petrosa ossis temporalis. Int. J. Legal Med. 114, 215–223. https://doi.org/10.1007/s004140000167.

Waltenberger, L., Rebay-Salisbury, K., Mitteroecker, P., 2021. Three-dimensional surface scanning methods in osteology: A topographical and geometric morphometric comparison. Am. J. Phys. Anthropol. 174, 846–858. https://doi.org/10.1002/ajpa.24204.